RVC OPEN ACCESS REPOSITORY – COPYRIGHT NOTICE

The full details of the published version of the article are as follows:

TITLE: Relationship Between Increased In Vivo Meniscal Loads and Abnormal Tibiofemoral Surface Alignment in ACL deficient Sheep is Varied

AUTHORS:
Beveridge, Jillian E.
Atarod, Mohammad
Heard, Bryan J.
O'Brien, Etienne E. J.
Frank, Cyril B.
Shrive, Nigel G.

Royal
Veterinary
College
University of London

Relationship Between Increased In Vivo Meniscal Loads and Abnormal Tibiofemoral Surface Alignment in ACL deficient Sheep is Varied

Jillian E. Beveridge, Post-Doctoral Fellow
Department of Orthopaedics, Warren Alpert Medical School, Brown University / Rhode Island Hospital
Bioengineering Labs, Coro West, Suite 404
Rhode Island Hospital
1 Hoppin Street, Providence, RI   02903
Ph: (401) 444-7180, Fax: (401) 444-4418, email: jillian_beveridge@brown.edu

Mohammad Atarod, Post-Doctoral Fellow
McCaig Institute for Bone and Joint Health, University of Calgary

Bryan J. Heard, Post-Doctoral Fellow
Department of Surgery
McCaig Institute for Bone and Joint Health, University of Calgary

Etienne E. J. O'Brien, D.V.M., Ph.D.
Royal Veterinary College of London

Cyril B. Frank, Professor*
Department of Surgery
McCaig Institute for Bone and Joint Health, University of Calgary

Nigel G. Shrive, Professor
Department of Civil Engineering
McCaig Institute for Bone and Joint Health, University of Calgary

*Deceased

Word Count: 3981

1

Abstract

The aim of this study was to quantify how abnormal dynamic tibiofemoral surface alignment affects the load bearing function of menisci in vivo. Using a sheep model of ACL deficiency, we tested the hypothesis that increased in vivo meniscal loads correlate with greater tibiofemoral surface alignment abnormality. Stifle kinematics were recorded using a bone-mounted instrumented spatial linkage in four sheep before, and at four and twenty weeks (w) after ACL transection. A parallel robotic manipulator was used to quantify stifle kinetics by reproducing each animal's in vivo kinematics and measuring tissue loads during gait. Meniscal resultant loads were estimated from the change in joint reaction force after sequentially removing load-bearing tissues. Tibiofemoral subchondral surfaces were then traced and modeled using thin plate splines. Proximity disturbance is a surface interaction measure used to quantify dynamic tibiofemoral surface alignment abnormality. ACL transection increased meniscal loads by 30-145% at 20w post-ACL transection, whereas the degree of dynamic tibiofemoral subchondral surface alignment varied between sheep. Positive and significant correlations between increased meniscal loads and proximity disturbance values >10mm were observed (R^2=0.04-0.57; p≤0.05). Our results suggest that the proximity disturbance measure reflects abnormal meniscal loads following ACL injury; however given the range of R^2 values, perturbations in dynamic tibiofemoral subchondral surface alignment do not explain abnormal joint kinetics entirely, and point to the presence of other dynamic compensatory mechanisms that may have a significant bearing on in vivo joint function and long-term joint health.

Introduction

Much work has been done to understand the biomechanical consequences of anterior cruciate ligament (ACL) deficiency, with the view to understand what constitutes abnormal motion, and then to use this knowledge in order to restore joint function as closely as possible in the hope that post-traumatic osteoarthritis (PTOA) can be attenuated (Lohmander, et al., 2007). Many have hypothesized that loads borne by the remaining structures of the knee are different following ACL tear (Frank, et al., 2004). By and large, in vitro (Allen, et al., 2000; Papageorgiou, et al., 2001) and numerical (Li, et al., 2002) studies have provided significant evidence to support the hypothesis. In vitro robotic studies in particular have demonstrated that the medial collateral ligament (MCL) and menisci function as secondary restraints to anterior tibial translation during a simulated motion path (Allen, et al., 2000; Kanamori, et al., 2000). Menisci also play a critical role in distributing contact stress uniformly between the tibiofemoral surfaces of the knee (Shrive, et al., 1978) and in modulating fluid flow within the load-bearing cartilage regions (Adeeb, et al., 2004). Thus impaired meniscal function is likely to result in joint instability and damage to the underlying articular cartilage (Englund and Lohmander, 2004). Despite the known consequences of impaired meniscal function, monitoring the presence of either impaired or abnormal dynamic function in vivo, and the relationship to PTOA onset, has been challenging.

Six degree of freedom (6-DOF) tibiofemoral kinematic abnormalities have been well characterized in both ACL-deficient humans (DeFrate, et al., 2006) and in large animal models of ACL injury (Tapper, et al., 2008; Tashman, et al., 2004). More recently, the term "surface interactions" has been adopted to describe the dynamic motion and alignment of tibiofemoral surfaces, and are believed to play a critical role in PTOA pathogenesis (Andriacchi, et al., 2009). Our group recently introduced a measure of dynamic tibiofemoral alignment in a sheep model of combined ACL and MCL transection. We termed the surface interaction "proximity disturbance" because it captures the change in distance between opposing tibiofemoral surfaces across a

region of near proximity (Beveridge, et al., 2014). That is, injury resulted in some tibiofemoral regions moving much closer together, and other regions moving farther apart. The greater this spread in change in proximity over a smaller contact area common to both intact and post-injury time points, the larger the proximity disturbance value (Figure 1). Thus proximity disturbance is a combined measure that quantifies changes in the complex tibiofemoral surface alignment, and is related to contact location and the individual's unique tibiofemoral surface geometry. Importantly, we showed that the severity of cartilage damage 20 weeks post-ACL/MCL transection in a sheep model is associated with larger proximity disturbance values. At the time, we hypothesized that proximity disturbance may reflect the loading environment of the joint, and could be related to the redistribution of contact stresses within the joint. Because the menisci play a key role in modulating contact stress, meniscal loads may be particularly sensitive to changes in dynamic tibiofemoral surface alignment.

Quantifying how abnormal dynamic tibiofemoral surface alignment affects the load bearing function of menisci would be a first step towards establishing a means to identify and monitor the presence of mechanisms believed to contribute to PTOA initiation in vivo. Using a sheep model of ACL deficiency, we tested the hypothesis that increased in vivo meniscal loads correlate with greater proximity disturbance values.

Methods

In vivo kinematics: Four skeletally mature female Suffolk-cross sheep were halter broken and trained to walk on a treadmill at a standardized speed of 0.9 m/s. Sheep were exercised at least thrice weekly, which consisted of 40 minutes of over ground and treadmill walking. Four weeks prior to kinematic measurement, modified fracture plates (Zimmer, Warsaw, IN, USA) were surgically affixed to the distolateral aspect of the hind right femur, and the proximolateral aspect of the hind right tibia to accommodate a custom removable plate-post assembly (Tapper, et al., 2004). At the time of kinematic collection, the rigid removable posts were secured to the

4

implanted facture plates, and an instrumented spatial linkage (ISL) was mounted to the posts.

The ISL consists of six rotational encoders, providing 6-DOF to its motion (accuracy =

0.3°/0.3mm), and has been described in detail previously (Rosvold, et al., 2015). Using the ISL,

in vivo kinematics were recorded prior to surgical intervention (Intact), and longitudinally at 4

and 20 weeks (w) post-operatively. At each kinematic session, approximately 200 strides were

collected. Surgical intervention consisted of arthroscopic transection of the hind right ACL, also

described in detail previously (Atarod, et al., 2014a). Following the final 20-week in vivo

kinematics measurement, animals were euthanized via intravenous injection (Euthanyl, Bimeda-

MTC, Cambridge, ON), and hind limbs disarticulated at the hip. All animal procedures were

approved by our institutional animal care committee and comply with the Canadian Council on

Animal Care guidelines.

Meniscal resultant loads: All soft tissues surrounding the stifle were dissected, save the

collateral and cruciate ligaments, and menisci. With the ISL attached, the stifle joint was

mounted in a unique 6-DOF parallel robot (R2000-PRSCo, NH, USA; 0.05mm accuracy) by

fixing the tibia to a custom fixture equipped with a 6-DOF force/moment sensor (1N/0.1Nm

accuracy; Omega 160, ATI Industrial Automation Apex, NC), and the femur to the robot end-

effector. A custom-made humidity chamber that surrounded the stifle was used to maintain a

consistent level of tissue hydration and temperature throughout mechanical testing. The robot

was then programmed to move the femur relative to the tibia while the ISL provided real-time

feedback to its control system such that in vivo stifle kinematics of a single real stride that was

closest to the average kinematics of the ~200 collected strides at each time point (i.e., Intact, 4

and 20w) were reproduced nearly exactly (reproduction accuracy=0.1°/0.1mm, (Atarod, et al.,

2014a)). Resultant stifle forces were recorded throughout the reproduced gait cycles that were

specific for each time point via the force/moment sensor in the custom tibial fixture. The load

borne by the menisci for each time point (Intact, 4 and 20w post-transection) was determined

using the principle of superposition by sequentially removing each of the stifle structures (Woo,

et al., 1999), and recording the change in resultant stifle load between successive kinematically identical gait cycles that are unique to each animal at each time point (Figure 2). Stifle structures were removed in the following order: MCL, lateral collateral ligament, posterior cruciate ligament, lateral meniscus, and medial meniscus.

Proximity disturbance (PD): A detailed description of PD determination is available in the Appendix, and in (Beveridge, et al., 2014). Briefly, the thin (<1mm) ovine tibiofemoral cartilage was removed and the subchondral surfaces were traced manually with a hand-held coordinate measuring machine (CMM) (Faro, FL, USA, accuracy=0.025mm). A thin plate spline was then fitted to the 3D subchondral surface point clouds (Beveridge, et al., 2013; Beveridge, et al., 2014). The size of the resulting rectangular mesh that we used to model the tibiofemoral surfaces was 0.50 x 0.50mm. Tibiofemoral proximity was calculated for each of the four tibiofemoral surfaces (medial tibial plateau (MTP) and femoral condyle (MFC), and lateral tibial plateau (LTP) and femoral condyle (LFC)), and proximity disturbance calculated using the methodology described in Figure 1. Using less accurate video-based motion capture methods, we have shown previously that PD precision is 2.6mm, or equal to roughly half of the inter-animal PD variation in uninjured sheep (Beveridge, et al., 2014). Please refer to the Appendix for additional details on the Proximity Disturbance metric.

Statistics: Using PD and meniscal load data from the entire stride (101 points corresponding to 0-100% Gait), linear regression was used to test for significant correlations between PD (independent variable) and changes in meniscal load (dependent variable). Separate regressions were carried out for each tibiofemoral surface and each sheep. Because the number of degrees of freedom in a statistical model with n=4 was insufficient to test for significant differences in regression slopes (β) across animals, β coefficients ± 95% confidence intervals (CIs) were plotted to visualize the degree that slopes varied between subjects. Correlations were considered significant if p≤0.05.

Results

Four-week data for Subject #3 were not collected due to lameness, which had resolved by 20w. ACL transection increased meniscal loads for all subjects except for Subject #1 at 4w (Figure 3 A & B). By 20w, meniscal loads were increased in all sheep during mid-stance (mid-stance occurs at ~30% gait; Figure 3 C & D). Increased meniscal loads correspond to increases of 30 - 145% over intact stifle meniscal loads at mid-stance at 20w. ACL transection also affected tibiofemoral proximity, with the greatest changes occurring at 20 weeks (Figure 4). ACL deficiency did not perturb kinematics equally across subjects, with one animal exhibiting minimal change in tibiofemoral proximities (Subject #1, Figure 4), and one animal exhibiting increases and decreases in proximities of approximately ± 6mm (Subject #4, Figure 4). The other two animals exhibited intermediary tibiofemoral proximity changes (Subjects 2 & 3, Figure 4). Proximity disturbance was calculated from the range in proximity values and proximity areas (Figure 1), and assessed relative to the increases in meniscal forces. The strength of these correlations between increased meniscal forces and proximity disturbance values ranged from significant negative correlations, to significant positive correlations (Table 1 & Figure 6). The negative correlations were present in subjects with minimal kinetic and kinematic changes (Subject 1, Figure 5), whereas the positive correlations were present in subjects with greater increases in meniscal loads and proximity disturbance values (Subject 4, Figure 5). The direction and strength for the two sheep with intermediary kinematic changes fell in between the two extremes shown by Subjects #1 and #4.The strength of the regression R^2 values and β coefficients were variable between subjects and over time (Figure 6), but were positive and with stronger R^2 values at 20w in 50% of the tibiofemoral surfaces (Table 1). Further, medial compartment R^2 values were consistently stronger than lateral compartment values.

7

Discussion

We sought to determine whether altered meniscal loads correlated with abnormal tibiofemoral surface alignment in ACL deficient sheep. Our results demonstrated that ACL transection led to greater meniscal resultant loads in all animals (shown previously in Atarod et al., 2015), but the direction and strength of the correlation was time and subject-specific, with significant correlations being more predominant at the 20w post-injury time point, and being positive only when stifle kinematics were more abnormal during weight-bearing. Therefore, our hypothesis was partially supported, and abnormal dynamic surface alignment does not explain increased meniscal loads entirely.

We have previously described that meniscal loads are coupled with anterior tibial translation both in the intact state, and following ACL transection: an increase in anterior tibial translation of several millimeters during weight acceptance increased meniscal loads dramatically for some animals – on the order of two to three times normal intact values (Atarod, et al., 2015). Results of this previous work support the accepted paradigm that menisci function as secondary restraints to anterior tibial translation, and may be at greater risk of injury due to larger load magnitudes following ACL injury (Allen, et al., 2000; Musahl, et al., 2010; Wieser, et al., 2011).

Although abnormal anterior tibial translation is a clear indicator of abnormal in vivo dynamic joint function both in large animal models (Mansour, et al., 1998; Tapper, et al., 2008; Tashman, et al., 2004) and in humans (Chen, et al., 2011; Papannagari, et al., 2006), the coupled nature of 6-DOF tibiofemoral motion means that changes in one degree affect the remaining degrees of freedom to some extent (Atarod, et al., 2014a; Wilson, et al., 2000). Therefore, small changes across multiple degrees of freedom, in addition to anterior tibial translation, may also impact tibiofemoral contact mechanics negatively; however, small changes in six measures of motion are difficult to relate to specific mechanical mechanisms that damage articular cartilage and contribute to PTOA initiation and progression. These shortcomings led us to develop the

8

proximity disturbance metric, which is a measure of how much injury disturbs normal joint surface alignment (Beveridge, et al., 2014). In a more unstable combined ACL and MCL transection model (ACL/MCLx), we showed that the severity of gross cartilage damage observed 20 weeks post-injury correlates with increased proximity disturbance values (Beveridge, et al., 2014). At that time, we speculated that proximity disturbance is likely related to the contact stresses between the articulating surfaces of the knee – including the interface between meniscus and cartilage. The positive correlation between increased meniscal loads and larger proximity disturbance values of the current study lend support to this hypothesis, although it is important to note that this relationship was not universal across all subjects as demonstrated by the variation in regression model β coefficients in Figure 6. Nevertheless, it stands to reason that if meniscal loads are greater in ACL deficiency, the loads transferred to the articular cartilage are also likely increased, and could be damaging to cartilage. Cadaveric (Imhauser, et al., 2013; McCarthy, et al., 2013) and numerical analyses (Li, et al., 2002) that have shown changes in contact stress distribution during a simulated ACL-deficient motion further support the assertion that abnormal kinematics increases contact stress between the meniscus-cartilage interface of the tibial plateau. Our in vivo results in Figure 4 indicate that the anterior regions of the femoral condyles and posterior regions of the tibial plateaus are in greater proximity at mid-stance following ACL transection, which could be indicative that contact stress is elevated in these regions. However, the menisci could also redistribute the load in a way that transfers increased contact stress to areas more distant from the localized apposing tibiofemoral surfaces in greater proximity. Future investigation that maps in vivo chondral changes alongside proximity disturbance, meniscal function, and joint kinetics measures is likely to yield valuable insight into the relationship between proximity disturbance, meniscal loads, and the spatial distribution of chondral changes following ACL injury.

Proximity disturbance magnitudes of the ACLx sheep were less than those of the more unstable ACL/MCLx model reported previously (peak PD values for ACL/MCLx: 40-60mm)

(Beveridge, et al., 2014). Because combined ACL/MCL transection creates a more unstable joint, it is not unexpected that the degree of dynamic tibiofemoral surface alignment abnormality is greater following combined ligament transection than following isolated ACL transection. In comparison, we have shown that proximity disturbance values of sheep that receive an open arthrotomy alone (all other joint structures are left intact) remain below 10mm (Beveridge, et al., 2014). Importantly, these sham-operated animals do not go on to develop OA-like changes 20w post-arthrotomy. In the current study, positive correlations between increased meniscal loads and proximity disturbance values emerged when proximity disturbance during stance exceeded 10mm. The presence of negative correlations between meniscal loads and proximity values (Table 1) resulted from meniscal loads and small PD values fluctuating in opposite directions within the gait cycle (e.g., Subject #1, Figure 5), and were observed in sheep that exhibited minimal changes in joint surface alignment. Taken collectively, our results suggest that a "safe" proximity disturbance threshold may exist that, once exceeded, joint kinetics are adversely affected and cartilage damage is likely to develop.

We also observed that medial compartment R^2 values were consistently greater than those of the lateral compartment (Table 1). Magnitudes of neither meniscal resultant loads nor proximity disturbance values seem to explain this trend. Femoral condyle, tibial plateau, and menisci geometries are different between medial and lateral compartments of the ovine stifle (Allen, et al., 1998; Osterhoff, et al., 2011; Proffen, et al., 2012), so perhaps an interaction exists amongst these geometries, alignment and meniscal function that is not obvious from our current data. Numerical models based on subject-specific tissue and osseous geometries, kinematics and kinetics that examine the soft tissue behavior of the cartilage and menisci may be a useful approach to examine these hypothesized interactions more deeply.

A key outcome of this investigation was that there was significant individual variability in the kinematic response to identical ACL transection procedures (Figure 4), but nearly ubiquitous increases in meniscal resultant loads by 20w post-ACL transection (Figure 3). While this inter-

10

subject variability in ACLx kinematics is consistent with previous kinematic studies in sheep (Frank, et al., 2012; Tapper, et al., 2004), and recapitulates the functional variability observed in human ACL deficiency (von Porat, et al., 2006), other dynamic mechanisms not captured by the proximity disturbance metric must also be modulating meniscal resultant loads. Co-contraction of knee flexor agonist and antagonist muscle groups would improve joint stability by way of increasing functional joint stiffness, and could explain the increased meniscus loads observed in these animals (Liu and Maitland, 2000; Tsai, et al., 2012). Coordination of agonist and antagonist muscle activation may also contribute to the smaller oscillations in both proximity disturbance values and meniscal loads that are apparent throughout the gait cycle (Figures 2 & 5). Muscles that act to provide joint stability could be firing at low load and frequencies in order to correct the joint position throughout gait. The variability of within-subject R^2 values and β coefficients over time further supports our speculation that some animals were able to adapt functionally to ACL deficiency: R^2 values that became weaker or negative over time as result of decreasing PD values suggests that dynamic surface alignment became more "normal" over time. Contrary to our hypothesis, abnormal in vivo joint kinetics – increased meniscal resultant loads, specifically – can be present with or without abnormal dynamic surface alignment. It is unclear what effect prolonged increased meniscal loading with near normal dynamic surface alignment will have on long-term joint health; however, our previous study in the ACL/MCLx model (Beveridge, et al., 2014) suggests that the presence of abnormal dynamic surface alignment is certainly detrimental. Future investigations that incorporate measures of neuromuscular control in tandem with in vivo kinetic, kinematic, and surface interaction measures will allow us to tease apart the interplay of these mechanical mechanisms and their contributions to PTOA pathogenesis.

We acknowledge that our study has several limitations. The use of a large animal model and the technical challenge of the approach itself limited the number of animals included; however, by using each animal as its own internal control and by implementing a repeated measures

design, we increased the statistical power to detect meaningful relationships between dynamic tibiofemoral surface alignment and meniscal function. Nevertheless, inclusion of more animals would add more confidence to our findings and would allow us to apply more sophisticated statistical analyses to define a proximity disturbance threshold that accurately predicts meniscal resultant loads and to test whether slopes of the meniscal force-PD regression models are different between animals. Answers to these questions would help establish thresholds for clinically meaningful associations. We also acknowledge that all kinetic measures, including "Intact" measures, were reproduced at 20w post-injury. It is possible that the material properties and geometries of the remaining tissues changed over time in response to mechanical and biological perturbations of the stifle milieu (Frank, et al., 2004; Funakoshi, et al., 2007; Mow, et al., 2005; Ochi, et al., 1997). This could mean that Intact and 4w meniscal force measures may not reflect the earlier time point function exactly. If cartilage and menisci had become more compliant over the 20w time frame, true meniscal forces would have been greater at earlier time points, thereby reducing the magnitude of the calculated change in post-operative meniscal loads. However, the total load borne by menisci at the Intact time point as a percentage of body mass of the four ACLx sheep of the current study are comparable to those of uninjured sheep measured using identical methods (ACLx = 68-87% vs uninjured = 53-71% body mass) (Rosvold, et al., 2016). Therefore, we have reason to believe that the magnitude of change in the mechanical properties of the menisci in this injury model remains subtle at 20w, with limited effect on our estimates of Intact meniscal loads.

Although gross meniscal damage or cartilage loss was not noted in any of the stifles at the time of sacrifice, it is also possible that subtle changes in these soft tissue geometries occurred, and could have influenced our results. Future studies that monitor stifle tissue morphology are needed to determine the natural history of stifle cartilage, osseous and meniscus geometry changes within the 20-week post-injury timeframe in this large animal model.

12

A limitation of the superposition technique in estimating resultant meniscal loads is that the boundary conditions of load-bearing cartilage are different following complete meniscectomy. In the absence of a meniscus, the cartilage regions normally compressed by the meniscus could expand, and lead to a small increase in cartilage-cartilage contact area. This increase in cartilage-cartilage area would allow more load to be transferred across the joint, and ultimately reduce the proportion of resultant joint load attributed to menisci load-bearing. Conversely, fluid support may be reduced in the absence of a meniscus, and reduce cartilage load-bearing capability, leading to an overestimation of meniscal resultant load. The reader is referred to the Appendix where a detailed discussion and illustration of these phenomena is provided. Despite these limitations, the superposition approach is the only indirect technique that does not require inserting a device directly into joint or tissue to record loads of in vivo gait cycles reproduced by the robot.

Although changes in tissue hydration could affect the viscoelastic behaviour of the stifle soft tissues ex vivo, we believe that these effects would not have influenced our conclusion for two reasons: 1) a humidity chamber was employed throughout the ex vivo robotic mechanical testing procedure to prevent tissue dehydration; and 2) if changes in tissue hydration impacted resultant load measures significantly, the bias was likely consistent between subjects because the testing protocol was systematic.

Lastly, the sheep stifle is not identical to the human knee, but it does exhibit many aspects of human PTOA following ACL injury and is a reasonable anatomical approximation of the human joint (Allen, et al., 1998; Osterhoff, et al., 2011). With respect to meniscal function specifically, the material properties of sheep menisci are most similar to those of human in comparison to other animal models (bovine, porcine, canine, and monkey) (Joshi, et al., 1995).

Our study also had several strengths. In contrast to existing studies that have investigated the load bearing function of menisci at discrete flexion angles within simulated or passive motion paths (Allen, et al., 2000; Papageorgiou, et al., 2001), our data are based on subject-specific in

13

vivo joint kinematics for an actual gait stride. Given that we have previously shown that perturbations of only 0.5mm in subject-specific gait paths can increase tissue loads by up to 100% (Atarod, et al., 2014b; Darcy, et al., 2007), we believe that using subject-specific in vivo motion as input to our mechanical testing platform is critically important if are to quantify in vivo meniscal function accurately. Our approach is therefore unique, and provides new insight into the sensitivity of joint kinetics to perturbations in in vivo joint kinematics and to other mechanisms that may modulate tissue loads independently of abnormal dynamic surface alignment. We also were able to assess changes in joint function relative to the intact state, which eliminates the use of the contralateral limb as a baseline measure. Lastly, we related the change in meniscal function to a surface interaction measure that we know is related to increased cartilage damage (Beveridge, et al., 2014). Future investigations that incorporate simultaneous measures of contact stress would allow us to test the hypothesis directly that increased proximity disturbance values are a reasonable surrogate for tibiofemoral contact stress.

In conclusion, we showed that increased in vivo meniscal loads correlate with greater proximity disturbance values in some, but not all, ACL-transected sheep. Our results suggest that the kinematic proximity disturbance measure can reflect abnormal joint kinetics, and abnormal meniscal loads specifically; however, perturbations in dynamic tibiofemoral surface alignment do not explain the increase in meniscal loads entirely, and point to the presence of other dynamic compensatory mechanisms that may have a significant bearing on in vivo joint function and long-term joint health.

Acknowledgements

Conflict of Interest Statement

None of the authors have received financial support from affiliations that may be perceived as having biased the presentation of the data.

References

Adeeb, S.M., Ahmed, E.Y.S., Matyas, J., Hart, D.A., Frank, C.B. and Shrive, N.G., 2004. Congruency effects on load bearing in diathrodial joints. Computer Methods in Biomechanics and Biomedical Engineering 7, 147-157.

Allen, C.R., Wong, E.K., Livesay, G.A., Sakane, M., Fu, F.H. and Woo, S.L., 2000. Importance of the medial meniscus in the anterior cruciate ligament-deficient knee. J Orthop Res 18, 109-115.

Allen, M.J., Houlton, J.E.F., Adams, S.B. and Rushton, N., 1998. The surgical anatomy of the stifle joint in sheep. Veterinary Surgery 27, 596-605.

Andriacchi, T.P., Koo, S. and Scanlan, S.F., 2009. Gait mechanics influence healthy cartilage morphology and osteoarthritis of the knee. J Bone Joint Surg Am 91 Suppl, 95-101.

Atarod, M., Frank, C.B. and Shrive, N.G., 2014a. Kinematic and Kinetic Interactions During Normal and ACL-Deficient Gait: A Longitudinal In Vivo Study. Ann Biomed Eng. 42, 566-578. doi: 510.1007/s10439-10013-10914-10433. Epub 12013 Sep 10418.

Atarod, M., Frank, C.B. and Shrive, N.G., 2015. Increased meniscal loading after anterior cruciate ligament transection in vivo: a longitudinal study in sheep. Knee. 22, 11-17. doi: 10.1016/j.knee.2014.1010.1011. Epub 2014 Nov 1018.

Atarod, M., Rosvold, J.M., Frank, C.B. and Shrive, N.G., 2014b. A Novel Testing Platform for Assessing Knee Joint Mechanics: A Parallel Robotic System Combined with an Instrumented Spatial Linkage. Ann Biomed Eng 12, 12.

Beveridge, J.E., Shrive, N.G. and Frank, C.B., 2013. Repeatability and precision of a weighted centroid method for estimating dynamic in vivo tibiofemoral surface interactions in sheep. Computer Methods in Biomechanics and Biomedical Engineering 17, 1853-1863.

Beveridge, J.E., Heard, B.J., Shrive, N.G. and Frank, C.B., 2014. A new measure of tibiofemoral subchondral bone interactions that correlates with early cartilage damage in injured sheep. Journal of Orthopaedic Research 32, 1371-1380.

Chen, C.H., Li, J.S., Hosseini, A., Gadikota, H.R., Gill, T.J. and Li, G., 2011. Anteroposterior stability of the knee during the stance phase of gait after anterior cruciate ligament deficiency. Gait and Posture

Darcy, S.P., Rosvold, J.M., Beveridge, J.E., Corr, D.T., Sutherland, C.A., Brown, J.J., Marchuk, L.L., Frank, C.B. and Shrive, N.G., 2007. Estimation of In-Vivo Forces During Gait In an Ovine Stifle Joint Requires Motion Reproduction to an accuracy of Less Than 0.5 mm. Journal 7, 1-67.

DeFrate, L.E., Papannagari, R., Gill, T.J., Moses, J.J., Pathare, N.P. and Li, G., 2006. The 6 degrees of freedom kinematics of the knee after anterior cruciate ligament deficiency. Am J Sports Med 34, 1240-1246.

Englund, M. and Lohmander, L.S., 2004. Risk factors for symptomatic knee osteoarthritis fifteen to twenty-two years after meniscectomy. Arthritis Rheum 50, 2811-2819.

Frank, C.B., Shrive, N.G., Boorman, R.S., Lo, I.K. and Hart, D.A., 2004. New perspectives on bioengineering of joint tissues: joint adaptation creates a moving target for engineering replacement tissues. Annals of Biomedical Engineering 32, 458-465.

Frank, C.B., Beveridge, J.E., Huebner, K.D., Heard, B.J., Tapper, J.E., O'Brien, E.J. and Shrive, N.G., 2012. Complete ACL/MCL deficiency induces variable degrees of instability in sheep with specific kinematic abnormalities correlating with degrees of early osteoarthritis. J Orthop Res 30, 384-392.

Funakoshi, Y., Hairu, M., Tapper, J.E., Marchuk, L.L., Shrive, N.G., Kanaya, F., Rattner, J.B., Hart, D.A. and Frank, C.B., 2007. Periarticular ligament changes following ACL/MCL transection in an ovine stifle joint model of osteoarthritis. Journal of Orthopaedic Research 25, 997-1006.

Imhauser, C., Mauro, C., Choi, D., Rosenberg, E., Mathew, S., Nguyen, J., Ma, Y. and Wickiewicz, T., 2013. Abnormal tibiofemoral contact stress and its association with altered kinematics after center-center anterior cruciate ligament reconstruction: an in vitro study. Am J Sports Med 41, 815-825.

Joshi, M.D., Suh, J.-K., Marui, T. and Woo, S.L.-Y., 1995. Interspecies variation of compressive biomechanical properties of the meniscus. Journal of Biomedical Materials Research 29, 823-828.

Kanamori, A., Sakane, M., Zeminki, J., Rudy, T.W. and Woo, S.L.Y., 2000. In-situ force in the medial and lateral structures of intact and ACL-deficient knees. J Orthop Sci 5, 567-571.

Li, G., Suggs, J. and Gill, T., 2002. The Effect of Anterior Cruciate Ligament Injury on Knee Joint Function under a Simulated Muscle Load: A Three-Dimensional Computational Simulation. Annals of Biomedical Engineering 30, 713-720.

Liu, W. and Maitland, M.E., 2000. The effect of hamstring muscle compensation for anterior laxity in the ACL-deficient knee during gait. Journal of Biomechanics 33, 871-879.

Lohmander, L.S., Englund, M., Dahl, L.L. and Roos, E.M., 2007. The long-term consequence of anterior cruciate ligament and meniscus injuries. Am J Sports Med 35, 1756-1769.

Mansour, J.M., Wentorf, F.A. and Degoede, K.M., 1998. In vivo kinematics of the rabbit knee in unstable models of osteoarthrosis. Annals of Biomedical Engineering 26, 353-360.

McCarthy, M.M., Tucker, S., Nguyen, J.T., Green, D.W., Imhauser, C.W. and Cordasco, F.A., 2013. Contact stress and kinematic analysis of all-epiphyseal and over-the-top pediatric reconstruction techniques for the anterior cruciate ligament. Am J Sports Med 41, 1330-1339.

Mow, V.C., Gu, W.Y. and Chen, F.H., 2005. Structure and Function of Articular Cartilage and Meniscus. Journal 181-258.

18

Musahl, V., Citak, M., O'Loughlin, P.F., Choi, D., Bedi, A. and Pearle, A.D., 2010. The effect of medial versus lateral meniscectomy on the stability of the anterior cruciate ligament-deficient knee. Am J Sports Med 38, 1591-1597.

Ochi, M., Kanda, T., Sumen, Y. and Ikuta, Y., 1997. Changes in the permeability and histologic findings of rabbit menisci after immobilization. Clinical Orthopaedics and Related Research 334, 305-315.

Osterhoff, G., Loffler, S., Steinke, H., Feja, C., Josten, C. and Hepp, P., 2011. Comparative anatomical measurements of osseous structures in the ovine and human knee. Knee 18, 98-103.

Papageorgiou, C.D., Gil, J.E., Kanamori, A., Fenwick, J.A., Woo, S.L. and Fu, F.H., 2001. The biomechanical interdependence between the anterior cruciate ligament replacement graft and the medial meniscus. Am J Sports Med 29, 226-231.

Papannagari, R., Gill, T.J., Defrate, L.E., Moses, J.M., Petruska, A.J. and Li, G., 2006. In vivo kinematics of the knee after anterior cruciate ligament reconstruction: a clinical and functional evaluation. Am J Sports Med 34, 2006-2012.

Proffen, B.L., McElfresh, M., Fleming, B.C. and Murray, M.M., 2012. A comparative anatomical study of the human knee and six animal species. Knee 19, 493-499.

Rosvold, J.M., Atarod, M., Frank, C.B. and Shrive, N.G., 2015. An instrumented spatial linkage for measuring knee joint kinematics. Knee

Rosvold, J.M., Atarod, M., Heard, B.J., O'Brien, E.J., Frank, C.B. and Shrive, N.G., 2016. Ligament and meniscus loading in the ovine stifle joint during normal gait. Knee 23, 70-77.

Shrive, N.G., O'Connor, J.J. and Goodfellow, J.W., 1978. Load-bearing in the knee joint. Clinical Orthopaedics and Related Research 131, 279-287.

Tapper, J., Ronsky, J., Powers, M., Sutherland, C., Majima, T., Frank, C. and Shrive, N., 2004. In vivo measurement of the dynamic 3-D kinematics of the ovine stifle joint. Journal of Biomechanical Engineering 126, 301-305.

Tapper, J., Fukushima, S., Azuma, H., Sutherland, C., Marchuk, L., Thornton, G., Ronsky, J., Zernicke, R., Shrive, N. and CB, F., 2008. Dynamic in vivo three-dimensional (3D) kinematics of the anterior cruciate ligament/medial collateral ligament transected ovine stifle joint. Journal of Orthopaedic Research 26, 660-672.

Tashman, S., Anderst, W., Kolowich, P., Havstad, S. and Arnoczky, S., 2004. Kinematics of the ACL-deficient canine knee during gait: serial changes over two years. Journal of Orthopaedic Research 22, 931-941.

Tsai, L.C., McLean, S., Colletti, P.M. and Powers, C.M., 2012. Greater muscle co-contraction results in increased tibiofemoral compressive forces in females who have undergone anterior cruciate ligament reconstruction. J Orthop Res 30, 2007-2014.

von Porat, A., Henriksson, M., Holmstrom, E., Thorstensson, C.A., Mattsson, L. and Roos, E.M., 2006. Knee kinematics and kinetics during gait, step and hop in males with a 16 years old ACL injury compared with matched controls. Knee Surg Sports Traumatol Arthrosc 14, 546-554.

Wieser, K., Betz, M., Farshad, M., Vich, M., Fucentese, S.F. and Meyer, D.C., 2011. Experimental loss of menisci, cartilage and subchondral bone gradually increases anteroposterior knee laxity. Knee Surg Sports Traumatol Arthrosc

Wilson, D.R., Feikes, J.D., Zavatsky, A.B. and O'Connor, J.J., 2000. The components of passive knee movement are coupled to flexion angle. J Biomech 33, 465-473.

Woo, S.L.-Y., Debski, R.E., Wong, E.K., Yagi, M. and Tarinelli, D., 1999. Use of Robotic Technology for Diathrodial Joint Research. Journal of Science and Medicine in Sports 2, 283-297.

Figure & Table Legends

Figure 1. Overview of each step in the Proximity Disturbance calculation. Black dots in the surface plots shown in (**B**) and (**D**) indicate locations of weighted centroids used to approximate regions of tibiofemoral proximity. Colour bar values are in mm and indicate the relative separation between tibiofemoral surfaces in (**B**) and the change in proximity in (**D**). Figure from Beveridge et al. (2014), with permission.

Figure 2. Schematic of the superposition method used to derive meniscal resultant loads.

Figure 3. Change in medial (A, C) and lateral (B, D) meniscal resultant loads during an in vivo gait cycle at 4 and 20 weeks (w) post-ACL transection. Mid-stance occurs at ~30% Gait.

Figure 4. Change in tibiofemoral proximity at mid-stance 20 weeks post-ACL transection for each Subject. For each subject, the femoral condyles are shown above, with the adjacent tibial plateaus below. Anterior, posterior, medial and lateral orientations are denoted by the capital letters on the four-bar legend in the centre. Negative colour bar values indicate reduced joint space width, whereas positive values indicate joint space widening. Surface plots are 3D objects collapsed to 2D for illustration purposes. All values are in mm; scale bars are provided on the bottom left of the surface plots.

Figure 5. Correlations between increased meniscal forces and proximity disturbance were negative when proximity changes were minimal (Subject #1, left panels), and were positive when proximity changes were larger (Subject #4, right panels). The orientation and format of the proximity plots are the same as in Figure 3. MFC refers to Medial Femoral Condyles. Blue shading in the middle panels indicates "normal" PD range (Beveridge, et al., 2014).

Figure 6. Regression model slope coefficients (β) ± 95% Confidence Intervals for each subject where the β contributed significantly to the model (indicated by "*"). Lateral compartment β coefficients were not significant at 4 weeks (w) (see Table 1), and are not shown. Four-week data for Subject #3 were not collected due to lameness, which resolved by 20w.

Table 1. Regression R^2 coefficients between changes in meniscal loads and proximity disturbance values for each subject. MTP/LTP = Medial / Lateral Tibial Plateaus; MFC/LFC = Medial / Lateral Femoral Condyles. Four-week data for Subject #3 were not collected due to lameness, which resolved by 20 weeks (w).

		4w		20w		Strength of R^2		4w		20w		Strength of R^2
		R^2	p-value	R_2	p-value	over time		R^2	p-value	R^2	p-value	over time
MTP	Subject #1	0.12	p<0.001	0.06	p=0.01	↓	**MFC**	0.04	p=0.004	-0.21	p<0.001	↑**
	Subject #2	0.29	p<0.001	0.08	p=0.002	↓		0.05	p=0.002	-0.13	p<0.001	↑**
	Subject #3	-	-	0.14	p<0.001	N/A		-	-	0.34	p<0.001	N/A
	Subject #4	0.09	p=0.001	0.44	p<0.001	↑		-0.05	p=0.003	0.55	p<0.001	↑*
LTP	Subject #1	0.00	p=0.88	0.04	p=0.02	↑*	**LFC**	0.01	p=0.47	-0.14	p=0.01	↑**
	Subject #2	0.03	p=0.07	0.16	p<0.001	↑		0.03	p=0.06	0.00	p=0.57	↓
	Subject #3	-	-	0.00	p=0.24	N/A		-	-	0.00	p=0.93	N/A
	Subject #4	-0.01	p=0.47	0.57	p<0.001	↑*		0.00	p=0.94	0.40	p<0.001	↑*

* = +ve B sign change from 4 to 20w
** = -ve B signchange from 4 to 20w

Figures & Tables

A. Subchondral bone surfaces are modeled and positioned in their *in vivo* orientation. Femoral (top) and tibial (bottom) surface models are shown in the frontal plane.

B. Inter-surface proximity is mapped at each surface face pre- and post-operatively. Femoral (top) and tibial models (bottom) are shown as if the models in (A) are opened so that the model surfaces (in grey in A) are facing out of the page. Anterior, posterior, medial, and lateral directions are noted with capital letters in the legend to the left of each model.

C. Proximity dataset overlap is determined. An example of tibial plateau proximity regions at Intact (red shading), 20w post-injury (blue shading), and overlapping regions (purple shading). Tibial models are in the same orientation as (B); femoral dataset overlap is determined using the same approach, but not shown here for simplicity.

$$\frac{\Delta proximity_{max} - \Delta proximity_{min}}{(overlapping\ proximity\ area\ /\ surface\ area)}$$

E. Proximity disturbance is calculated as the range of change in proximity (mm) divided by the normalized overlapping proximity surfaces areas (mm^2/mm^2) (Equation 1). Proximity disturbance units are mm.

D. From overlapping datasets (purple shaded region in C), change in proximity (shown above, in mm), overlapping proximity area (mm^2), and total surafce area (mm^2) are determined for medial and lateral femoral (top) and tibial (bottom) surfaces. Surface models are shown in the same orientation as in (B).
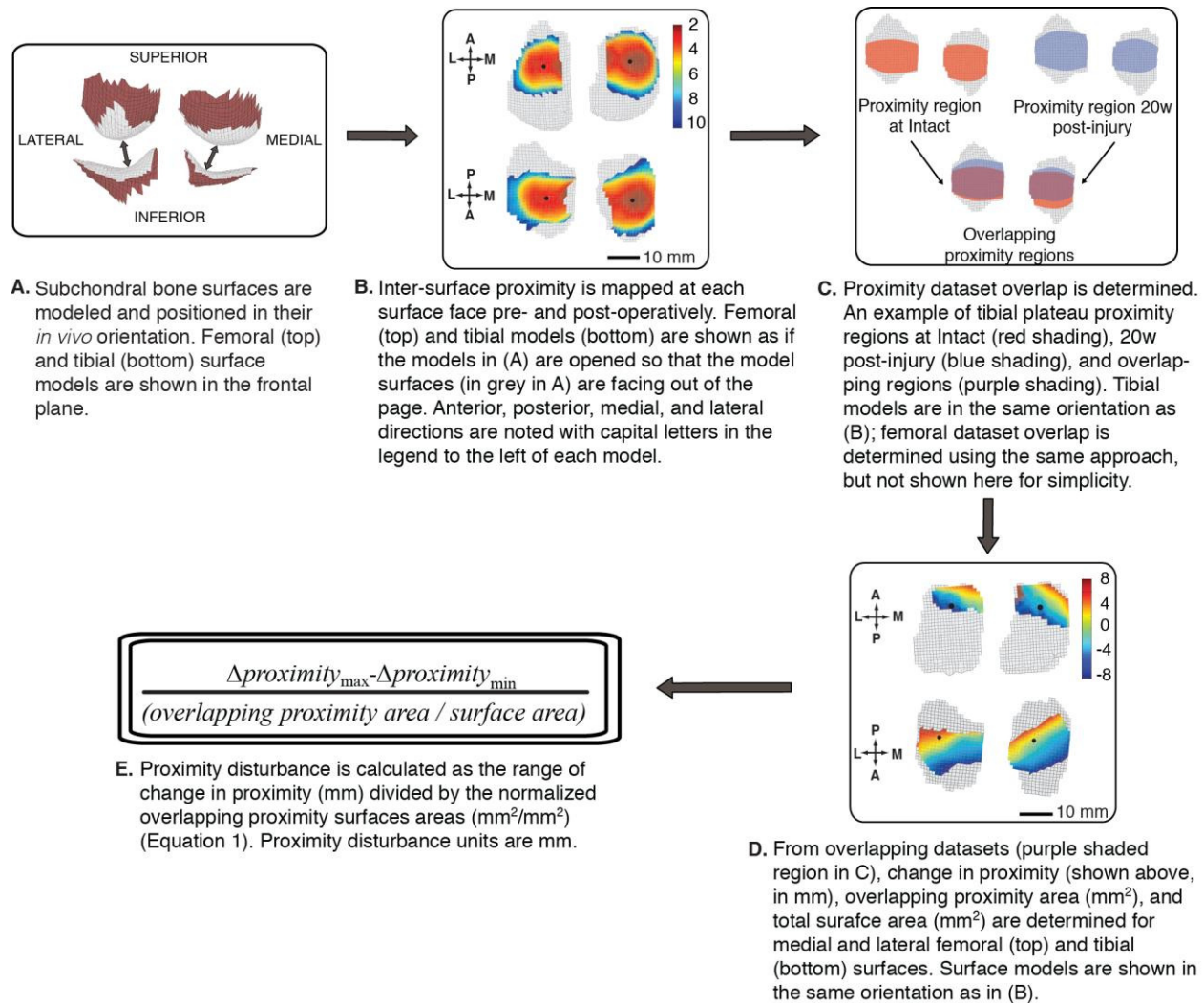
Figure 1. Overview of each step in the Proximity Disturbance calculation. Black dots in the surface plots shown in (**B**) and (**D**) indicate locations of weighted centroids used to approximate regions of tibiofemoral proximity. Colour bar values are in mm and indicate the relative separation between tibiofemoral surfaces in (**B**) and the change in proximity in (**D**). Figure from Beveridge et al. (2014), with permission.

21

Reproduce *Intact,*
4w & 20w in vivo motion
with all structures intact

Remove single
load-bearing tissue and
reproduce in vivo motion
for *each time point*

Record Joint Load
for *Intact, 4w, & 20w*
gait cycles
(Joint Load$_2$)

Record Joint Load
for *Intact, 4w, & 20w*
gait cycles
(Joint Load$_1$)

Remove single
load-bearing tissue and
reproduce in vivo motion
for *each time point*

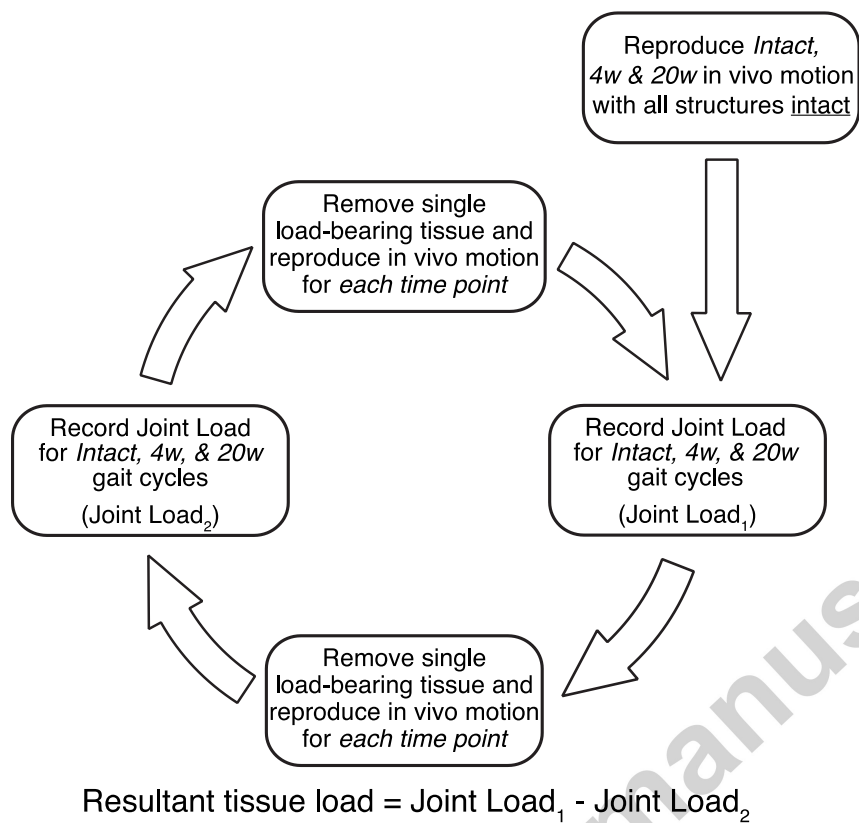Resultant tissue load = Joint Load$_1$ - Joint Load$_2$

Figure 2. Schematic of the superposition method used to derive meniscal resultant loads.
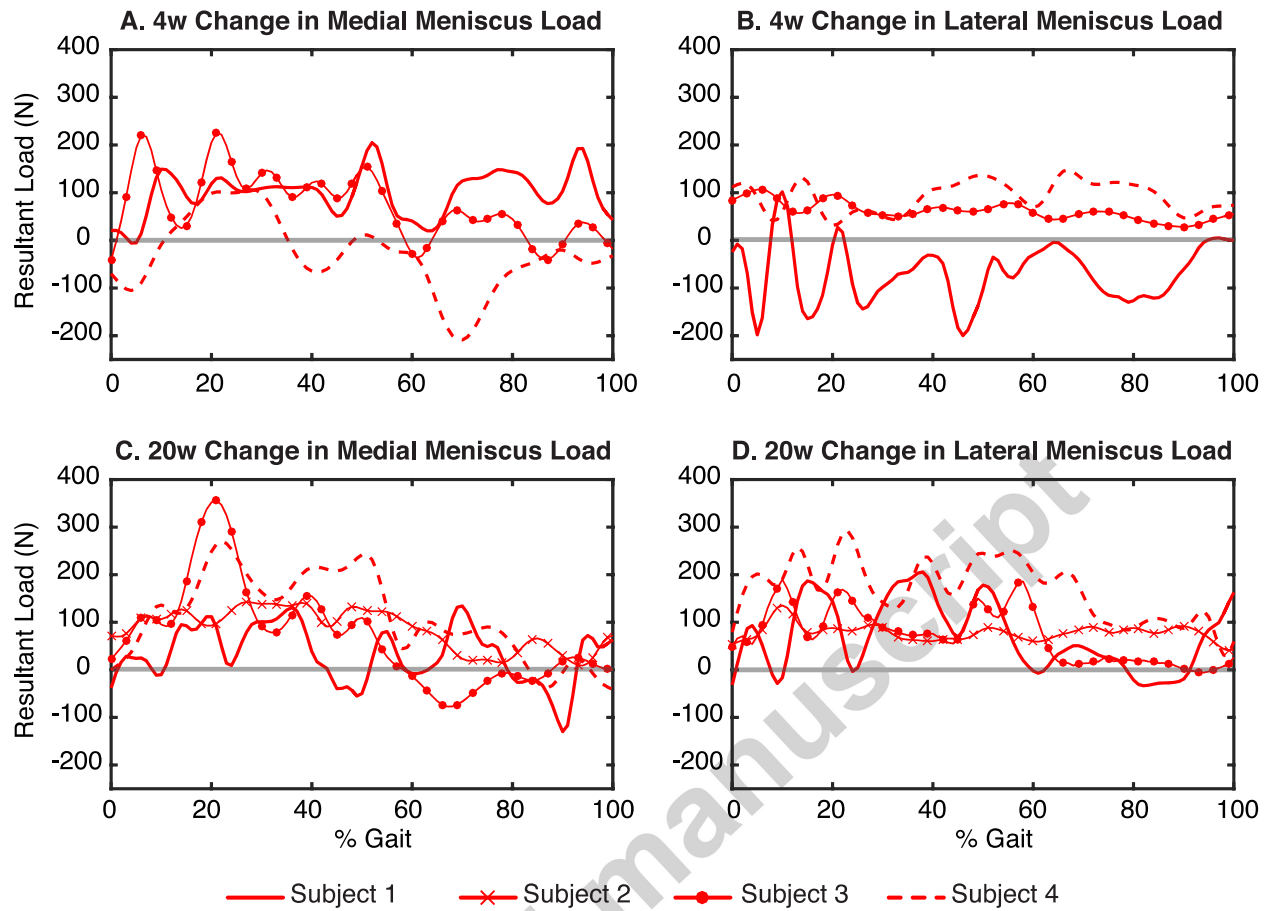
Figure 3. Change in medial (A, C) and lateral (B, D) meniscal resultant loads during an in vivo gait cycle at 4 and 20 weeks (w) post-ACL transection. Mid-stance occurs at ~30% Gait.

23

Figure 4. Change in tibiofemoral proximity at mid-stance 20 weeks post-ACL transection for each Subject. For each subject, the femoral condyles are shown above, with the adjacent tibial plateaus below. Anterior, posterior, medial and lateral orientations are denoted by the capital letters on the four-bar legend in the centre. Negative colour bar values indicate reduced joint space width, whereas positive values indicate joint space widening. Surface plots are 3D objects collapsed to 2D for illustration purposes. All values are in mm; scale bars are provided on the bottom left of the surface plots.
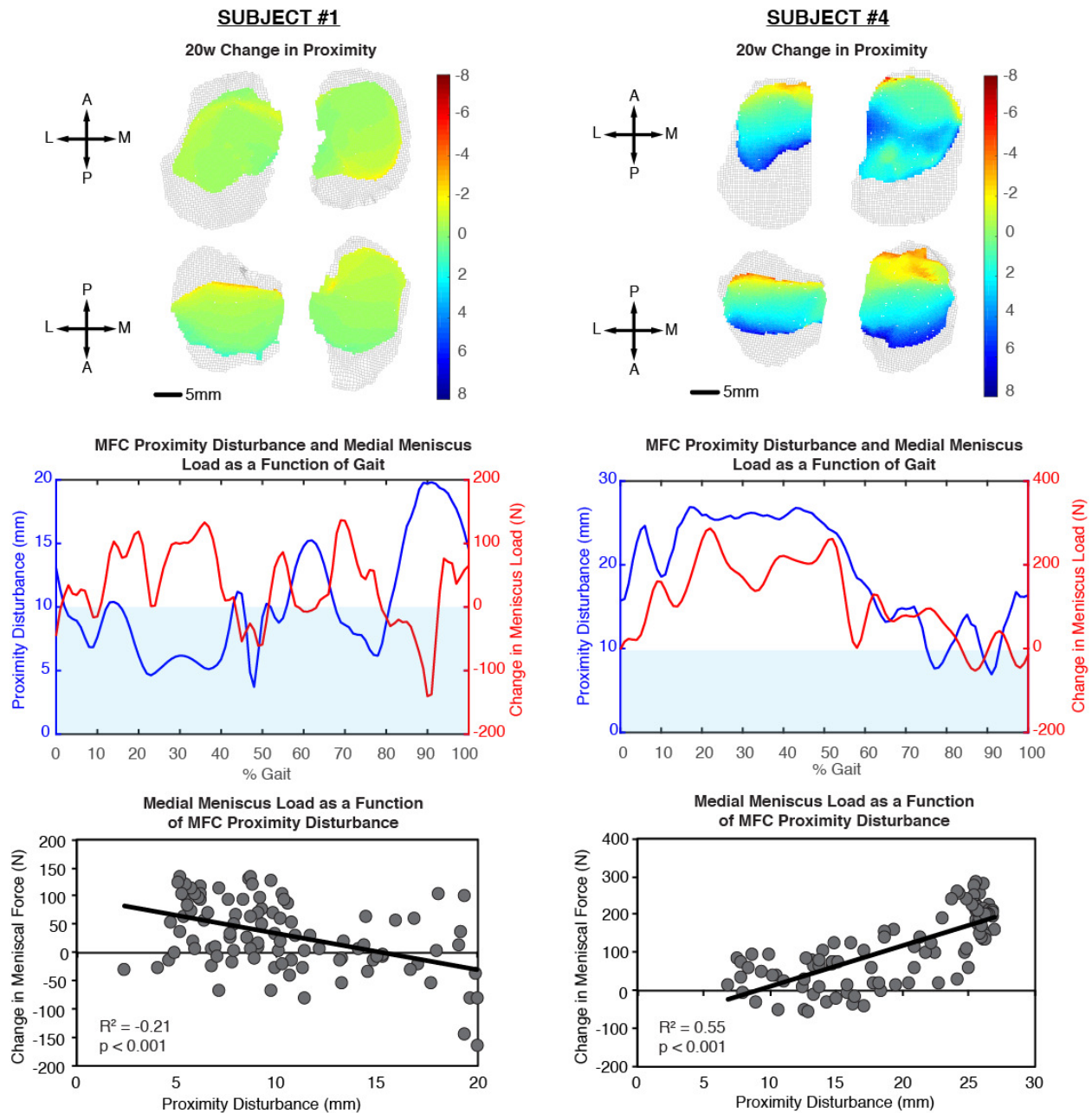
Figure 5. Correlations between increased meniscal forces and proximity disturbance were negative when proximity changes were minimal (Subject #1, left panels), and were positive when proximity changes were larger (Subject #4, right panels). The orientation and format of the proximity plots are the same as in Figure 3. MFC refers to Medial Femoral Condyles. Blue shading in the middle panels indicates "normal" PD range (Beveridge, et al., 2014).
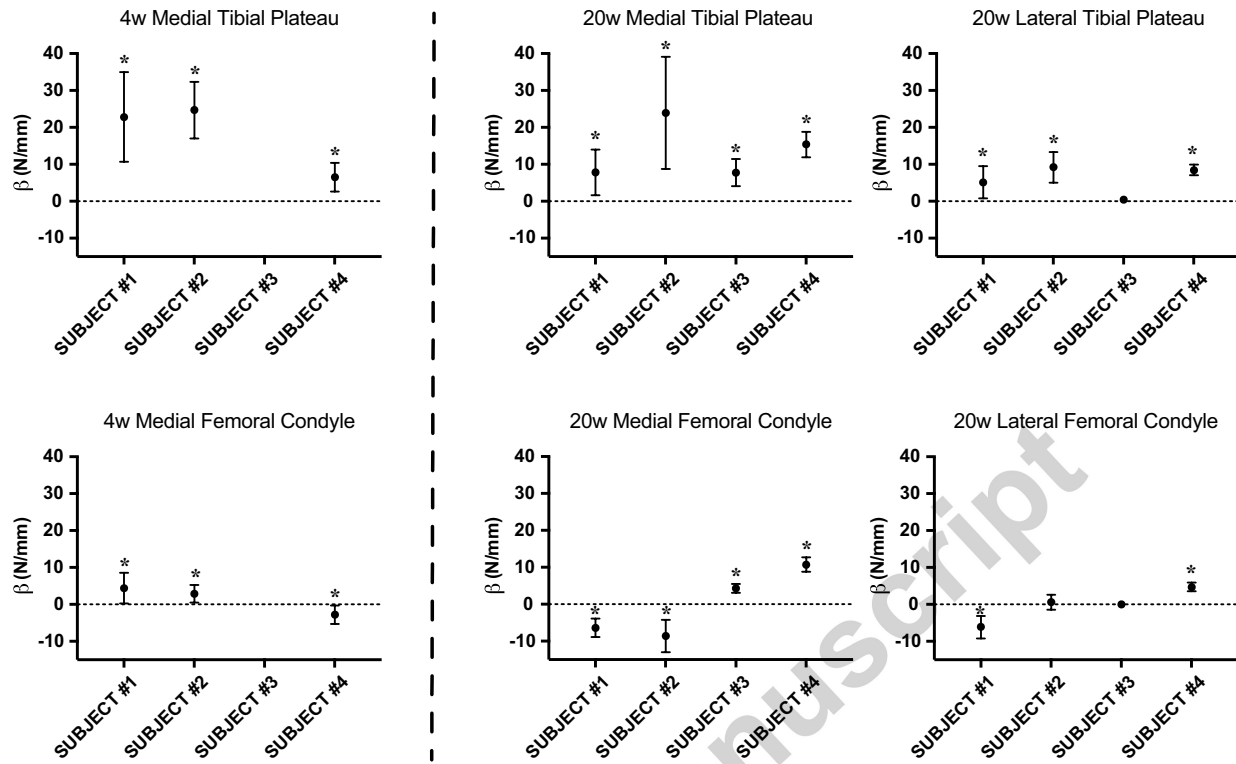
Figure 6. Regression model slope coefficients (β) ± 95% Confidence Intervals for each subject where the β contributed significantly to the model (indicated by "*"). Lateral compartment β coefficients were not significant at 4 weeks (w) (see Table 1), and are not shown. Four-week data for Subject #3 were not collected due to lameness, which resolved by 20w.